

A role for Schwann cell–derived neuregulin-1 in remyelination

Ruth M Stassart^{1,2,7}, Robert Fledrich^{1,7}, Viktorija Velanac^{1,3}, Bastian G Brinkmann^{1,4}, Markus H Schwab¹, Dies Meijer⁵, Michael W Sereda^{1,6} & Klaus-Armin Nave¹

After peripheral nerve injury, axons regenerate and become remyelinated by resident Schwann cells. However, myelin repair never results in the original myelin thickness, suggesting insufficient stimulation by neuronal growth factors. Upon testing this hypothesis, we found that axonal neuregulin-1 (NRG1) type III and, unexpectedly, also NRG1 type I restored normal myelination when overexpressed in transgenic mice. This led to the observation that Wallerian degeneration induced *de novo* NRG1 type I expression in Schwann cells themselves. Mutant mice lacking a functional *Nrg1* gene in Schwann cells are fully myelinated but exhibit impaired remyelination in adult life. We suggest a model in which loss of axonal contact triggers denervated Schwann cells to transiently express NRG1 as an autocrine/paracrine signal that promotes Schwann cell differentiation and remyelination.

In the peripheral nervous system, myelin is made by Schwann cells as a multilayered membrane sheath that provides electrical insulation and low-capacitance ensheathment of large-caliber axons for rapid impulse conduction^{1,2}. Myelin sheath thickness is proportional to fiber size, with a *g*-ratio (axon diameter/myelinated fiber diameter) of about 0.71 that provides optimal nerve conduction velocity. The underlying fine-tuning of myelin membrane growth is controlled by axonal signals^{1,3}, most notably by expression of the neuronal EGF-like growth factor NRG1 (refs. 4,5). During peripheral nerve development, neuronal NRG1 type III is the predominant isoform, regulating virtually all stages of the Schwann cell lineage, and the amount of axonally expressed NRG1 type III determines myelin sheath thickness^{3–7}. This interaction of axonal NRG1 type III with ERBB2 and ERBB3 receptor tyrosine kinases, expressed on Schwann cells and their precursors, is well understood^{6,7}.

However, the *Nrg1* gene encodes an entire family of more than 15 membrane-resident and secreted proteins^{6–8}, including that of NRG1 type I and II, which act as soluble signaling factors. Although these isoforms have also been detected in the peripheral nervous system (see below), their physiological function is unknown.

After nerve injury, Schwann cells have an important role for repair by contributing to the growth permissive environment that allows peripheral axons to regenerate⁹. At the same time, Wallerian degeneration (and the disintegration of axonal membranes) completely disrupts axon-Schwann cell contacts, which had persisted throughout normal development. Whereas ERBB2 is reportedly dispensable for Schwann cell survival and proliferation after injury¹⁰, Schwann cells redifferentiate and then remyelinate newly generated axons in a NRG1-dependent fashion^{11,12}.

After remyelination, the normal ratio between axon diameter and myelin sheath thickness is lost. By *g*-ratio analysis, the remyelinated axons are substantially hypomyelinated^{13,14}, but it is unclear why. Hypomyelination could be caused either by insufficient stimulation of redifferentiated Schwann cells or by inhibitory signals, or both. In addition, Schwann cells could have lost the ability to normally respond to myelination-inducing factors¹³. Using *Nrg1* transgenic (C57Bl6-Tg(*Thy1-Nrg1*III*)1*Kan*^{+/–} and C57Bl6-Tg(*Thy1-Nrg1*I*)1*Kan*^{+/–}, termed *Nrg1(I)* or *Nrg1(III)* tg mice, respectively⁴) and conditional *Nrg1* mutant mice (C57Bl6-Tg(*Dhh-cre*)1*Mejr* crossbred to C57Bl6-(*Nrg1*^{*tm2Cbm*}) mice, termed *Dhh-Cre* × *Nrg1*^{*loxP/loxP*} mice^{15,16}), we addressed the unresolved question of why Schwann cells do not regain the normal myelin sheath thickness after nerve injury^{13,14}.

Here we show that peripheral nerve remyelination was more efficient in mice overexpressing NRG1 type III (*Thy1-Nrg1(III)* tg mice) than in the wild type, but to our surprise this was also more efficient in mice overexpressing NRG1 type I (*Thy1-Nrg1(I)* tg mice). Additional analysis led to the finding that nerve injury triggered expression of NRG1 type I by Schwann cells, which is barely detectable in intact nerves. We demonstrate in a conditional mouse mutant that Schwann cell–derived NRG1 is essential for efficient peripheral nerve remyelination. This leads to a greatly expanded model of NRG1 in myelination control, which includes the autocrine stimulation of remyelination by Schwann cells that have transiently lost normal axonal contacts.

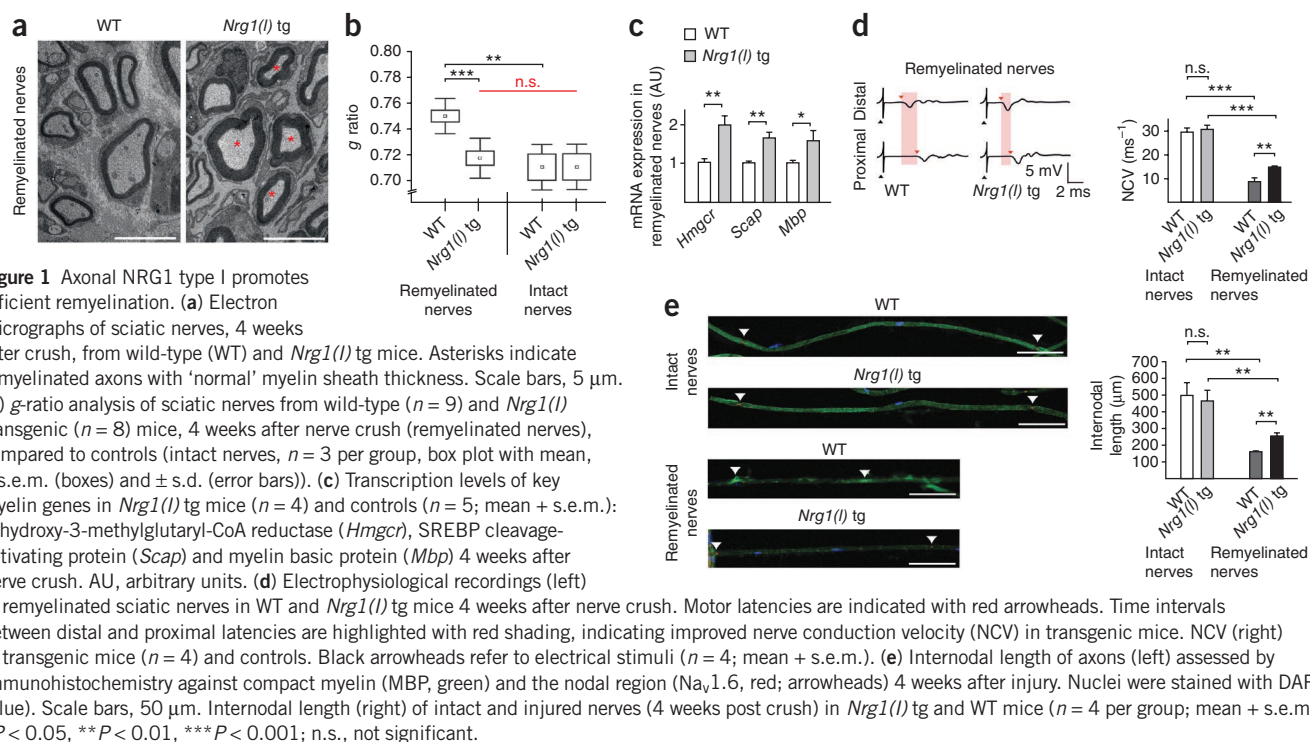
RESULTS

Neuronal NRG1 restores myelin thickness after injury

We first asked whether elevated neuronal (axonal) NRG1 expression could improve the incomplete remyelination typically observed after

¹Max Planck Institute of Experimental Medicine, Department of Neurogenetics, Göttingen, Germany. ²Department of Neuropathology, University of Göttingen, Göttingen, Germany. ³German Center for Neurodegenerative Diseases, Bonn, Germany. ⁴Department of Neurosurgery, Charité, University Medicine, Berlin, Germany. ⁵Department of Genetics, Erasmus Medical Center, Rotterdam, The Netherlands. ⁶Department of Clinical Neurophysiology, University of Göttingen, Göttingen, Germany. ⁷These authors contributed equally to this work. Correspondence should be addressed to M.W.S. (sereda@em.mpg.de) or K.-A.N. (nave@em.mpg.de).

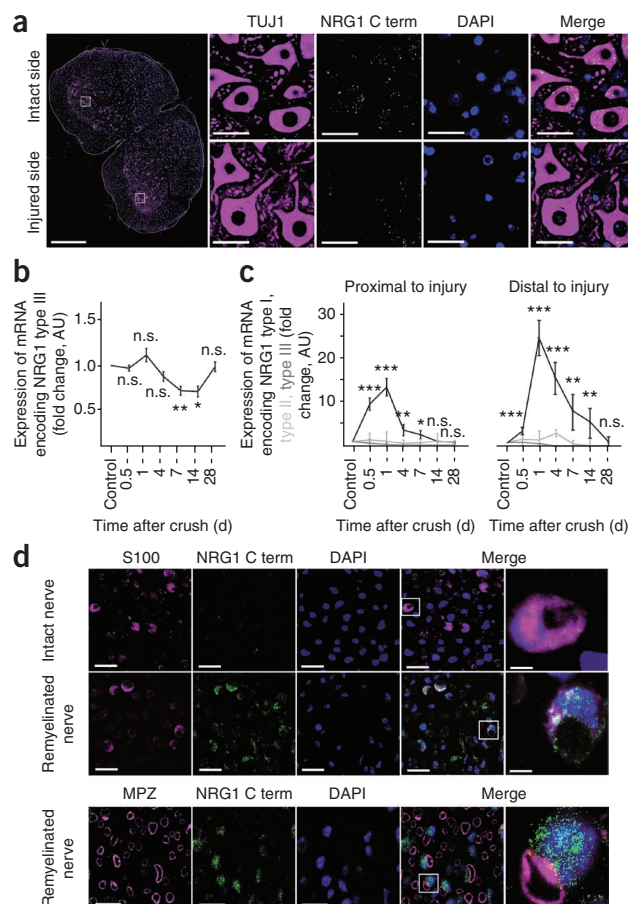
Received 2 October; accepted 15 November; published online 9 December 2012; doi:10.1038/nn.3281



peripheral nerve injury. To this end, we induced sciatic nerve crushes in mice that overexpress NRG1 type III under control of the neuronal *Thy1* promoter. This membrane-bound growth factor improved myelin thickness after repair, with *g* ratios resembling those observed during developmental hypermyelination⁴ (Supplementary Fig. 1a). Also, overexpressing the soluble NRG1 type I isoform in mice (which has no effect on normal myelination⁴) improved remyelination of crushed sciatic nerves. In these mice, 4 weeks after injury, the *g* ratios were indistinguishable from those in untreated (intact) wild-type or untreated *Nrg1(I)* transgenic mice (Fig. 1a,b and Supplementary Fig. 1b). In line with these histological observations, we determined an up to twofold increase of key regulators of myelin membrane biogenesis at the transcriptional level (Fig. 1c).

That nerve conduction velocity was not fully restored (Fig. 1d) is explained by reduced axonal calibers of the regenerated nerves at 4 weeks after injury, a finding independent of the genotype (Supplementary Fig. 1c,d). Nerve conduction velocity was presumably additionally reduced by the shortened internodal length

of remyelinated axons, which was only marginally improved in mice overexpressing NRG1 type I (Fig. 1e). This confirms that longitudinal myelin growth is not substantially regulated by NRG1 (ref. 4).



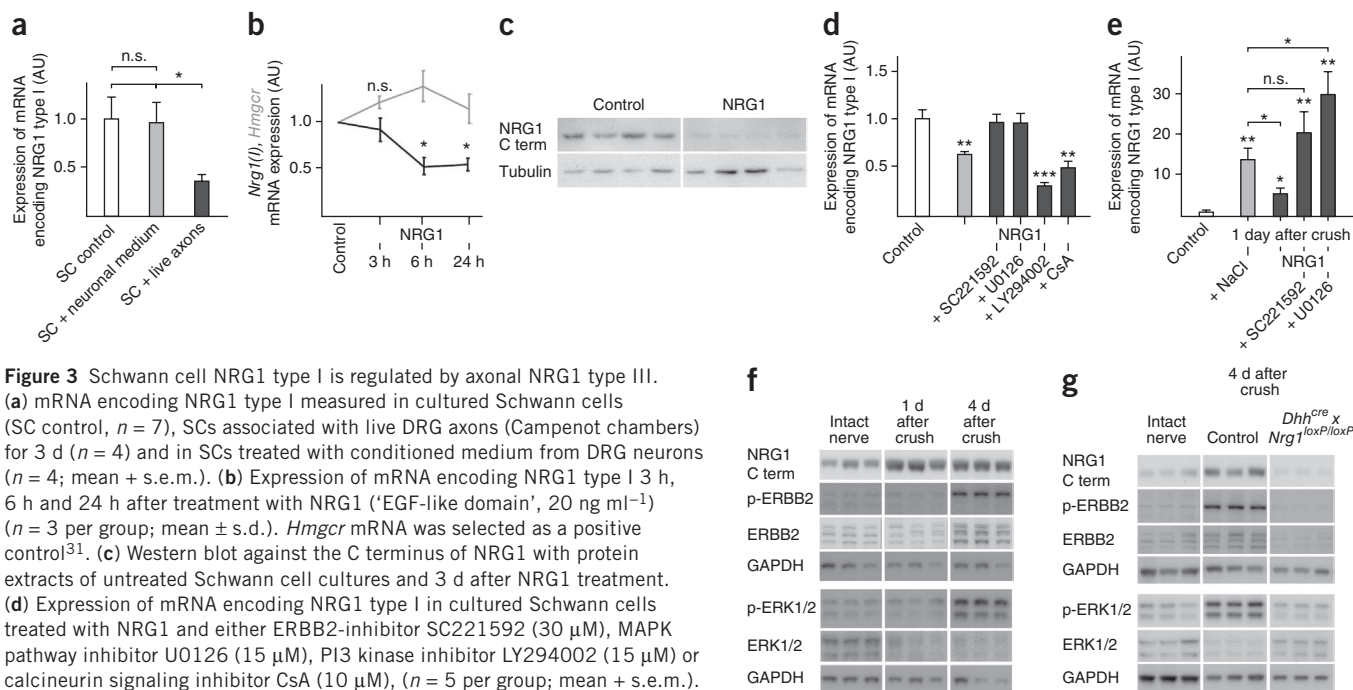


Figure 3 Schwann cell NRG1 type I is regulated by axonal NRG1 type III. (a) mRNA encoding NRG1 type I measured in cultured Schwann cells (SC control, $n = 7$), SCs associated with live DRG axons (Campenot chambers) for 3 d ($n = 4$) and in SCs treated with conditioned medium from DRG neurons for 3 d ($n = 4$; mean \pm s.e.m.). (b) Expression of mRNA encoding NRG1 type I 3 h, 6 h and 24 h after treatment with NRG1 ('EGF-like domain', 20 ng ml⁻¹) ($n = 3$ per group; mean \pm s.d.). *Hmgcr* mRNA was selected as a positive control³¹. (c) Western blot against the C terminus of NRG1 with protein extracts of untreated Schwann cell cultures and 3 d after NRG1 treatment. (d) Expression of mRNA encoding NRG1 type I in cultured Schwann cells treated with NRG1 and either ERBB2-inhibitor SC221592 (30 μ M), MAPK pathway inhibitor U0126 (15 μ M), PI3 kinase inhibitor LY294002 (15 μ M) or calcineurin signaling inhibitor CsA (10 μ M), ($n = 5$ per group; mean \pm s.e.m.). (e) Expression of mRNA encoding NRG1 type I in the distal sciatic nerve 1 d after injury (see also Fig. 2c). At the time of crush surgery, nerves were locally injected with saline (NaCl) or NRG1 (10 ng), either solely or with ERBB2 inhibitor (SC221592, 11.8 ng) or ERK1/2 inhibitor (U0126, 11.4 μ g) ($n = 4$ –5; mean \pm s.e.m.). (f) In intact and injured wild-type nerves, western blot analysis of NRG1 and ERBB2 and ERK1/2 phosphorylation. Axonal expression of NRG1 was barely detectable in sciatic nerve³². (g) Western blot of intact and injured nerves (in wild-type and *DhhCre* \times *Nrg1*^{loxP/loxP} mice) to analyze NRG1, ERBB2 and ERK1/2 phosphorylation. For full-length western blots see **Supplementary Figure 5**. * $P < 0.05$, ** $P < 0.01$, *** $P < 0.001$; n.s., not significant. AU, arbitrary units.

Tested molecular markers of Schwann cell proliferation (KI67) and differentiation (POU3F1, periaxin and EGR2) were unchanged at the RNA and protein level when quantified 2 weeks after crush, at the beginning of remyelination (**Supplementary Fig. 1e,f** and data not shown). Similarly, improved remyelination after injury was not associated with differences in Schwann cell number (**Supplementary Fig. 1g**).

Schwann cell-derived NRG1 is induced after nerve injury

As remyelinating Schwann cells did not lose their ability to respond to elevated expression of NRG1 in transgenic mice, an 'insufficient supply' of neuronal NRG1 could underlie hypomyelination after peripheral nerve injury. Schwann cells most likely lack stimulation by axonal NRG1 type III simply because of the loss of axonal contact during Wallerian degeneration¹⁷. Moreover, in wild-type motoneurons of the spinal cord, we detected a decrease of NRG1 expression 2 weeks after nerve crush, a time when axons regrow and become remyelinated^{17,18} (**Fig. 2a**). Expression of mRNA encoding NRG1 type III returned to normal about 4 weeks after crush (**Fig. 2b**). Consistently, transcription of *Nrg1* (III) in dorsal root ganglia (DRG) neurons transiently decreased after nerve injury, in line with previous observations¹⁹ (**Supplementary Fig. 2a**). Notably, in DRG neurons of mice overexpressing NRG1 type I, the temporal expression pattern of mRNA encoding NRG1 type III after nerve crush was indistinguishable from that in injured wild-type mice (**Supplementary Fig. 2b**).

In the course of these studies we also analyzed the proximal and distal compartment of crushed sciatic nerves and observed that expression of mRNA encoding NRG1 type I (but not type II or type III), was strongly induced in denervated Schwann cells (**Fig. 2c**)²⁰. Notably, the distal stump of the injured nerve demonstrated

a much stronger (about twofold) expression of mRNA encoding NRG1 type I compared to that in the proximal nerve segment (**Fig. 2c**). In this distal region, mRNA encoding NRG1 type I in Schwann cells was induced within 24 h and remained above normal until at least 2 weeks after crush, that is, during the dedifferentiation and early redifferentiation and remyelination period in Schwann cells^{17,18} (**Fig. 2c**). A corresponding increase in the amount of NRG1 protein in remyelinating Schwann cells was still detectable by immunofluorescence and western blot analysis 4 weeks after crush (**Fig. 2d** and **Supplementary Fig. 2c**).

Schwann cell NRG1 expression is controlled by axonal NRG1

We hypothesized that denervated Schwann cells contribute to remyelination by expression of NRG1 type I and autocrine stimulation after nerve injury, perhaps compensating for the lack of axonal contacts and insufficient supply of axonally presented NRG1 type III. Thus, we also hypothesized that Schwann cells might induce NRG1 expression in response to reduced exposure of axonal NRG1. Indeed, in adult mutant mice with a reduced expression of NRG1 type III (C57Bl6-*Nrg1*^{tm1Lwr}, termed *Nrg1* (III)^{+/-} mice here²¹), we observed an increase in Schwann cell-derived mRNA encoding NRG1 type I (**Supplementary Fig. 2d**). To study this dependency in detail, we took advantage of primary rat Schwann cell cultures. By mRNA expression in these (denervated) Schwann cells, mRNA encoding NRG1 type I was indeed the most abundantly expressed transcript (**Supplementary Fig. 2e**). We then compared the level of mRNA encoding NRG1 type I between primary rat Schwann cells in monocultures and Schwann cells exposed (for 3 d) to live axons obtained from cultured DRG neurons. Indeed, this axonal contact induced the downregulation of mRNA encoding NRG1 type I in cultured Schwann cells (**Fig. 3a**). Treatment of Schwann cells with conditioned medium from wild-type neurons did not notably affect

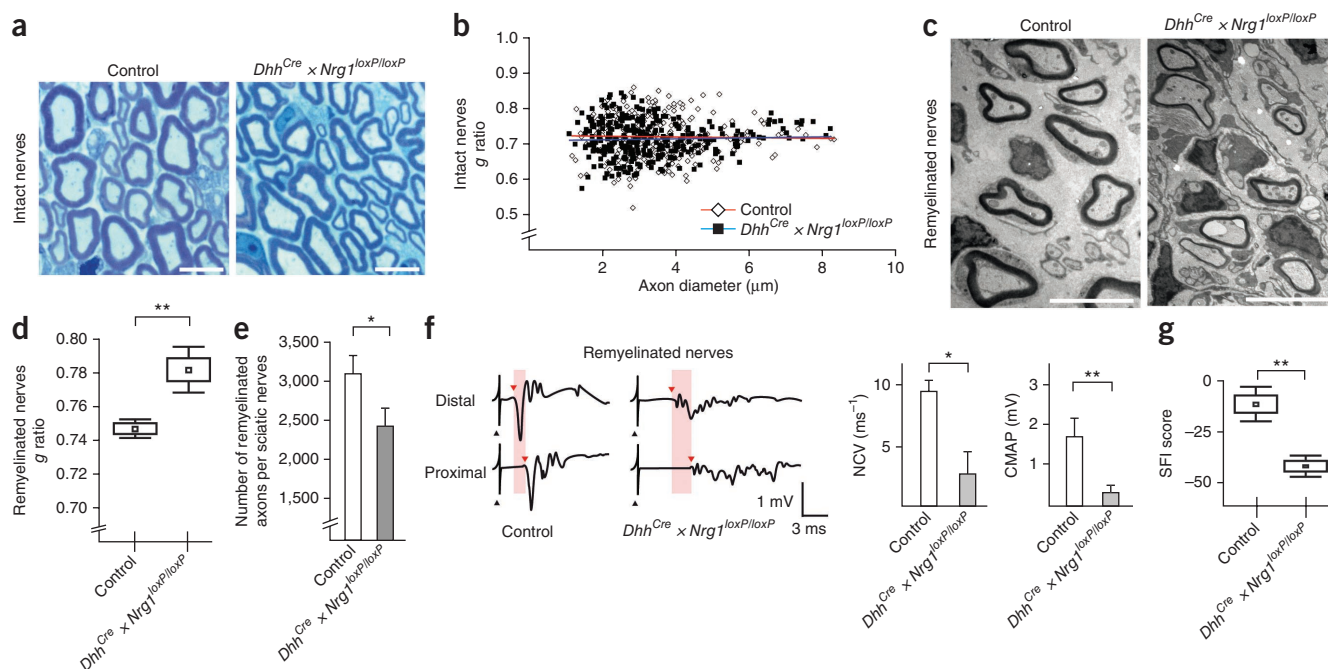


Figure 4 Schwann cell–derived NRG1 is required for efficient remyelination. **(a)** Light microscopy images of sciatic nerve cross-sections, showing normal myelination in mice with conditional ablation of *Nrg1* in Schwann cells (*Dhh^{Cre} × Nrg1^{loxP/loxP}* age 3 months). Scale bars, 7.5 μm. **(b)** Quantification of the data in **a** ($n = 3$ per group). **(c)** Electron micrographs of the sciatic nerve 4 weeks after crush, illustrating impaired remyelination in *Dhh^{Cre} × Nrg1^{loxP/loxP}* mice compared to injured controls (control; scale bars, 5 μm). **(d)** *g*-ratio analysis after remyelination ($n = 3$ –4; box plot with mean, \pm s.e.m. (boxes) and \pm s.d. (error bars)). **(e)** Quantification of regenerated axons after crush compared to controls ($n = 3$ per group; mean \pm s.e.m.). **(f)** Electrophysiological traces of sciatic nerves in control and *Dhh^{Cre} × Nrg1^{loxP/loxP}* mice 4 weeks after crush. Black arrowheads indicate electrical stimuli. Red arrowheads specify motor latencies. Time intervals between distal and proximal latencies are highlighted with red shading, indicating reduced nerve conduction velocity (NCV) in *Dhh^{Cre} × Nrg1^{loxP/loxP}* mice. Note the increased temporal dispersion of compound muscle action potentials in mutant mice. Quantification of data reveals a further reduced NCV (middle) and compound muscle action potentials (CMAP; right) in *Dhh^{Cre} × Nrg1^{loxP/loxP}* mice ($n = 3$) compared to controls ($n = 4$; mean \pm s.e.m.). **(g)** The sciatic nerve function index (SFI) demonstrates a severely impaired functional recovery of *Dhh^{Cre} × Nrg1^{loxP/loxP}* mice compared to controls 4 weeks after crush ($n = 3$ per group, box plot with mean, \pm s.e.m. (boxes) and \pm s.d. (error bars)).

mRNA encoding NRG1 type I (Fig. 3a). However, similar conditioned medium from neurons overexpressing NRG1 type I caused a significant ($P < 0.001$, two-tailed Student's *t* test) decrease in mRNA encoding NRG1 type I in Schwann cells (Supplementary Fig. 2f).

To determine whether neuronal NRG1, the key axonal regulator of Schwann cell differentiation, controls NRG1 expression *in trans*, we treated cultured Schwann cells with the recombinant (EGF-like) signaling domain common to all NRG1 isoforms. In these experiments, Schwann cells had reduced amounts of mRNA encoding NRG1 type I within 1 d after addition of the recombinant protein (Fig. 3b) and exhibited a clear decrease of NRG1 protein after 3 d (Fig. 3c). This NRG1-dependent inhibition of glial mRNA encoding NRG1 type I could be abolished by pharmacological inhibition of either the ERBB2 receptor or the ERK1/2 signaling pathway, but not by inhibition of PI3 kinase or calcineurin signaling (Fig. 3d).

To explore these mechanisms *in vivo*, we performed sciatic nerve crushes in wild-type mice and simultaneously applied NRG1 protein (that is, the soluble EGF-like domain) to the distal nerve segment, to test the hypothesis that exogenous NRG1 regulates *Nrg1* transcription in Schwann cells. One day after injury, exogenously supplied NRG1 had reduced Schwann cell mRNA encoding NRG1 type I by more than 50% (Fig. 3e). This inhibition by soluble NRG1 was abolished by concomitant application of ERBB2 or ERK1/2 inhibitors to the crushed nerve (Fig. 3e).

Next, we analyzed the temporal pattern of ERBB2 and ERK1/2 phosphorylation in the crushed sciatic nerve. After rapid phosphorylation of ERK1/2 (6 h after crush; Supplementary Fig. 2g), ERBB2

and ERK1/2 were strongly activated by 4 d, as previously reported^{20,22} (Fig. 3f). An increase of NRG1 protein was detected at 1 d and persisted for at least 4 weeks after crush (Fig. 3f and Supplementary Fig. 2c). This suggests that also the activation of ERBB2 and ERK1/2 is mediated by NRG1 released from resident Schwann cells. To test this hypothesis directly, we generated a mouse mutant (*Dhh-Cre × Nrg1^{loxP/loxP}* mice) lacking *Nrg1* expression selectively in Schwann cells (Fig. 3g). Four days after crush, ERBB2 and ERK1/2 phosphorylation were absent in these mutants (Fig. 3g).

Thus, we suggest a working model in which axonal NRG1 type III signaling to myelinating Schwann cells, mediated by ERBB receptors and the ERK1/2 signaling pathway, is a mechanism by which myelinated axons continuously suppress *Nrg1 type I* transcription in Schwann cells themselves. However, if 'derepressed' (after Wallerian degeneration with demyelination, Schwann cell dedifferentiation and the loss of axonal contact), an autocrine or paracrine NRG1 type I signaling by Schwann cells contributes to efficient remyelination after injury.

Schwann cell–derived NRG1 in remyelination

To determine *in vivo* whether NRG1 signaling by Schwann cells is indeed critical for efficient remyelination of injured nerves, we took advantage of the *Dhh-Cre × Nrg1^{loxP/loxP}* mice. Morphological analysis revealed no obvious defects of myelination (Fig. 4a), with normal *g* ratios and axonal size distribution (Fig. 4b). Thus, Schwann cell–derived NRG1 appears dispensable for primary myelination and myelin maintenance.

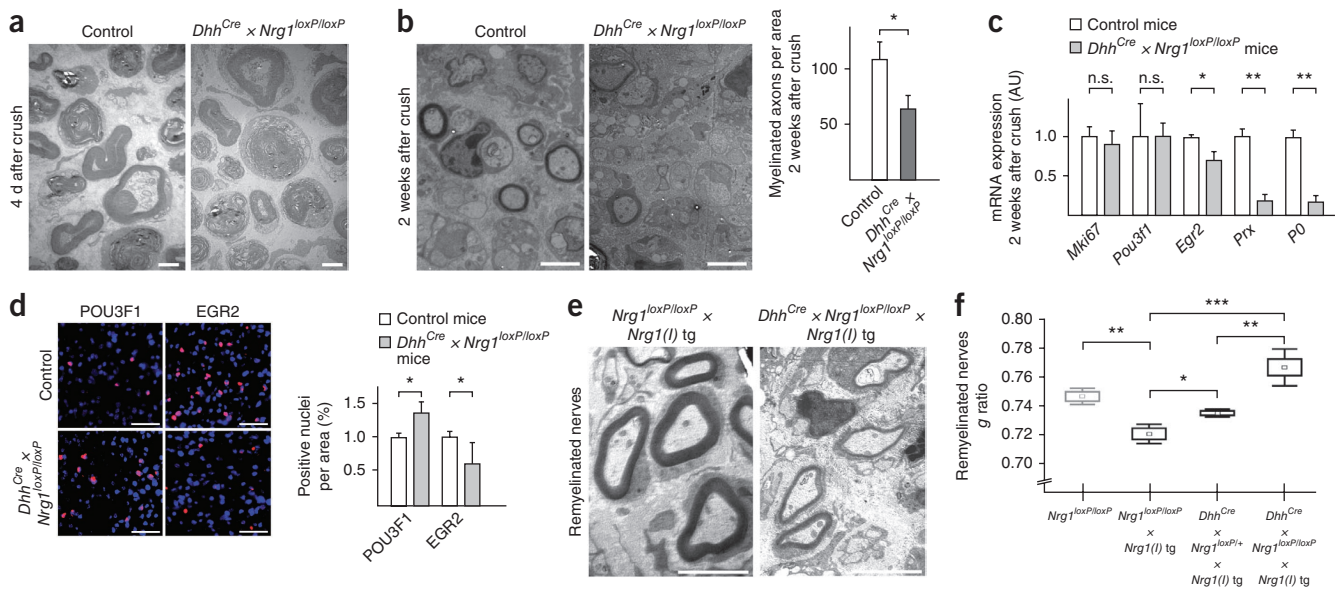


Figure 5 Schwann cells require NRG1 expression for timely redifferentiation. (a) Electron micrographs of the sciatic nerve 4 d after crush, illustrating an increased abundance of axonal degeneration profiles ('myelin balls') in *DhhCre* × *Nrg1*^{loxP/loxP} mice compared to controls. Scale bars, 2.5 μm. (b) Electron micrographs of the sciatic nerve 2 weeks after nerve crush, and quantification of remyelinated axons. Scale bars, 2.5 μm. *n* = 3; mean ± s.e.m. (c) Two weeks after crush, expression of late Schwann cell differentiation markers *Krox20* (*Egr2*), periaxin (*Prx*) and myelin protein zero (*Mpz*; also known as *P0*). Expression differences of the early proliferation marker *Ki67* (*Mki67*) and the transcription factor *Oct6* (*Pou3f1*) did not reach significance at the mRNA level (*n* = 4 per group; mean ± s.e.m.). AU, arbitrary units. (d) Immunohistochemistry analysis 2 weeks after crush in indicated mice for POU3F1-positive immature Schwann cells and KROX20 (*EGR2*)-expressing cells (*n* = 3 per group; mean ± s.e.m.). Scale bars, 20 μm. (e) Electron micrographs of remyelinated sciatic nerves from *DhhCre* × *Nrg1*^{loxP/loxP} mutants cross-bred to *Nrg1(I)* tg mice (right) and controls (left, *Nrg1*^{loxP/loxP} × *Nrg1(I)* tg) 4 weeks after nerve crush. Scale bars, 5 μm. (f) Quantification of the data in **e** by *g*-ratio analysis. *Nrg1*^{loxP/loxP} and *Nrg1*^{loxP/loxP} × *Nrg1(I)* tg, *n* = 3; *DhhCre* × *Nrg1*^{loxP/loxP} × *Nrg1(I)* tg, *n* = 3; *DhhCre* × *Nrg1*^{loxP/loxP} × *Nrg1(I)* tg, *n* = 5 (box plot with mean, ± s.e.m. (boxes) and ± s.d. (error bars)). **P* < 0.05, ***P* < 0.01, ****P* < 0.001; n.s., not significant.

In contrast, loss of NRG1 expression from Schwann cells strongly impaired remyelination after nerve crush, resulting in more severe hypomyelination than that observed for nerve regeneration of wild-type mice (Fig. 4c,d and Supplementary Fig. 3a,b). In addition, we noticed fewer myelinated axons in (remyelinated) sciatic nerves, together with more axons (>1 μm in diameter) that had remained completely unmyelinated (Fig. 4e and Supplementary Fig. 3c). The vast majority (83%) of these unmyelinated axons were associated with Schwann cells (Supplementary Fig. 3c). Schwann cell numbers 4 weeks after nerve crush were unaltered (Supplementary Fig. 3d).

After crush injury, electrophysiological recordings of the sciatic nerves in Schwann cell-specific *Nrg1* mutants revealed an additional reduction in nerve conduction velocity and in compound muscle action potentials compared to crush injury in control mice (Fig. 4f). Also the functional recovery of locomotion was severely impaired in *Dhh-Cre* × *Nrg1*^{loxP/loxP} mice, as measured by standardized walking analysis and calculation of the sciatic nerve functional index (Fig. 4g).

To explore the role of Schwann cell-derived NRG1 type I in the regenerating nerve, we analyzed axon breakdown and Schwann cell dedifferentiation (Fig. 5a and Supplementary Fig. 3e), which normally peaks 4 d after nerve injury^{17,18}. We observed more myelin-containing axon degeneration profiles ('myelin balls') in *Dhh-Cre* × *Nrg1*^{loxP/loxP} mutant mice, and it is plausible that upon axon injury Schwann cells dedifferentiate faster if they can not switch to NRG1 type I as an alternate autocrine/paracrine signal. However, the much larger number of (still) myelinated and (partially) degenerated axons was not different at 4 d (Fig. 5a and Supplementary Fig. 3e). In contrast, 2 weeks after injury, when in controls many more axons have regrown and become remyelinated^{17,18}, *Dhh-Cre* × *Nrg1*^{loxP/loxP} mutant mice exhibited fewer myelinated axons (Fig. 5b). Schwann cell

numbers and Schwann cell proliferation rates were not altered, as determined by *Mki67* mRNA quantification and KI67 immunostaining (Fig. 5c and Supplementary Fig. 3f,g). Only the number of cells expressing the transcription factor POU3F1, a marker of immature Schwann cells²³, was increased (Fig. 5d). In turn, an essential transcription factor of myelination, *EGR2*, and the myelin proteins periaxin and myelin protein zero were reduced in abundance in mutant nerves compared to controls (Fig. 5c,d). We conclude that NRG1 expression by Schwann cells is required for their own timely redifferentiation after axonal injury.

Finally, we asked whether the elevated expression of *Nrg1(I)* in neurons (which had also enabled 'complete' remyelination in transgenic mice) would rescue the poor remyelination that we observed in Schwann cell-specific *Nrg1* mutants. Notably, mRNA expression of Schwann cell-derived *Nrg1* after nerve crush was not different in these mutants compared to injured controls (Supplementary Fig. 4a). In the progeny of *Dhh-Cre* × *Nrg1*^{loxP/loxP} × *Nrg1(I)* tg mice, we assessed sciatic nerve remyelination after crush, and found this to be inefficient. Analysis of myelin sheath thickness revealed that these double mutants clearly did not remyelinate as efficiently as mice overexpressing NRG1 type I did (Fig. 5e,f and Supplementary Fig. 4b). Indeed, hypomyelination in these mice was closest to that in *Dhh-Cre* × *Nrg1*^{loxP/loxP} single mutants (Fig. 4c,d). Thus, in an experimental situation, neuronal NRG1 type I can promote efficient myelin repair, but it cannot compensate for the absence of *Nrg1* expression in Schwann cells.

DISCUSSION

We found that the regulation of myelin synthesis in Schwann cells, tightly controlled by the axonal growth factor NRG1 type III, becomes

more complex after nerve injury in adult mice. This happens when Schwann cells have dedifferentiated and are temporarily detached from the axons that have undergone Wallerian degeneration. The ability of these Schwann cells to induce their own *Nrg1* gene has emerged as critical for efficient remyelination. We showed that denervated Schwann cells express NRG1 type I, a soluble signaling protein, most likely triggered by the loss of axon contact and axonal NRG1 type III signaling (**Supplementary Fig. 4c**). Theoretically, demyelination and dedifferentiation may also contribute to increased NRG1 expression in Schwann cells after injury. However, we note that a reduced baseline expression of axonal NRG1 type III in mutant mice (*Nrg1(III)^{+/-}* mice) was sufficient to increase mRNA encoding NRG1 type I in Schwann cells. Moreover, the exposure to axonal membranes or the treatment with recombinant NRG1 protein were sufficient to suppress *Nrg1* expression by Schwann cells, *in vitro* and *in vivo*, and this downregulation required ERBB receptor functions and the MAPK pathway in Schwann cells. Finally, in transgenic mice with acute nerve injury, the neuronal overexpression of either NRG1 type I or type III strongly promoted the remyelination of axons, to the point that we measured 'normal' myelin sheath thickness. Thus, NRG1-ERBB signaling in peripheral nerves becomes complex after nerve injury and involves both axonal and Schwann cell-derived NRG1 isoforms.

Schwann cells are known to respond to peripheral nerve injury with a unique regenerative program. They demonstrate an exceptional plasticity in the nervous system, characterized by the ability to dedifferentiate and to convert into redifferentiating and remyelinating cells after nerve damage²⁴. In contrast, it is not obvious why myelin sheath thickness of regenerated axons remains reduced^{13,14} and why complete functional recovery after peripheral nerve trauma is rare²⁵.

That remyelination is not a simple recapitulation of nerve development has been clearly established in the recent years^{24,26}. Especially the dedifferentiation of Schwann cells has been characterized in detail, and factors that negatively regulate myelination have been identified^{23,24,27}. Remyelination, in contrast, depends on extracellular matrix compounds, neurotrophic factors and hormones^{3,25,26}. Factors that specifically drive Schwann cell redifferentiation and remyelination in adult nerves were previously not known. During normal development axonal NRG1 type III is crucial for Schwann cell proliferation, differentiation and myelination⁶. Our data suggest that the Schwann cell response to NRG1 differs in many ways after injury (compared to primary development). For example, lack of NRG1 signaling did not affect Schwann cell numbers after nerve crush, in agreement with normal proliferation of mature Schwann cells lacking ERBB2 receptors¹⁰. Indeed, after Wallerian degeneration, Schwann cells must proliferate in the absence of axons, and axons will regrow only after Schwann cells have formed longitudinal cell columns, the 'bands of Büngner'²⁶. Nevertheless, axonal NRG1 is required for remyelination¹¹.

Can reduced axonal NRG1 signaling after nerve injury account for incomplete remyelination^{13,14}? Neuronal overexpression of NRG1 type III restores myelin sheath thickness and even induces hypermyelination after nerve crush, demonstrating that Schwann cells are NRG1-responsive also in regenerating nerves. That also neuronal NRG1 type I overexpression rescues mice from inefficient myelin repair surprised us and was more difficult to understand because endogenous expression of NRG1 type I is low in DRG and motoneurons^{8,28}. Axonal NRG1 type I is a paracrine signaling molecule that reaches denervated Schwann cells easily at a distance and could simply mimic Schwann cell-derived NRG1 type I. However, neuronal overexpression of NRG1 type I cannot compensate for Schwann cell-derived

NRG1 type I, suggesting that neuronal and glial NRG1 functions are distinct in the course of myelin repair. We emphasize that Schwann cell-derived NRG1 type I is most prominent at early time points after injury, that is, when axons (and thus axonal NRG1 type III) are lost by Wallerian degeneration. Neuronal NRG1 overexpression is only functional when axons have regenerated and therefore specifically affects later stages of Schwann cell redifferentiation and remyelination. This may explain why neuronal NRG1 signaling can not fully 'compensate' for the absence of Schwann cell-derived NRG1 type I after injury (in *Thy1-Nrg1(I) tg × Dhh-Cre × Nrg1^{loxP/loxP}* mice), which remains essential for the initial steps of remyelination.

After Wallerian degeneration, Schwann cell redifferentiation begins in the absence of axonal NRG1 and may instead be controlled by Schwann cell autonomous factors. The amount of mRNA encoding NRG1 type I in Schwann cells was highest between days 1 and 4, when axons (and consequently axonal NRG1 type III) were absent from the distal stump. The induction of NRG1 type I in injured Schwann cells *in vivo* is likely related to the behavior of 'denervated' Schwann cells as observed in culture. Both axonal contact and the addition of recombinant NRG1 suppresses their endogenous NRG1 expression, and we suggest that axonal NRG1 also negatively regulates the expression of NRG1 type I in associated Schwann cells *in vivo*. Thus, NRG1 type I emerges as a cell-autonomous Schwann cell growth factor in the regenerating nerve. We note that aberrant stimulation of cell growth by autocrine or paracrine NRG1-ErbB signaling has been observed in Schwann cell cultures and in human Schwannomas^{29,30}, but the function of these signaling loops had remained obscure.

In line with our working model, mice deficient for NRG1 expression in Schwann cells had normal peripheral nerve development, demonstrating that Schwann cell-derived NRG1 is dispensable in the presence of axonal NRG1 type III. In contrast, after peripheral nerve crush, mice lacking NRG1 in Schwann cells exhibited severely impaired nerve regeneration. Thus, denervated Schwann cells require autocrine NRG1 type I signaling for timely redifferentiation, whereas neuronal NRG1 (specifically the axon-bound isoform) stimulates remyelination by itself.

Taken together, the redifferentiation of Schwann cells after nerve injury and the efficient remyelination of new axons occur in a critical time window, in which denervated Schwann cells are susceptible to growth-factor stimulation. We suggest that NRG1 expression, switching from neurons (axons) to Schwann cells (**Supplementary Fig. 4c**), is required for efficient myelin repair and thus constitutes an endogenous regulator of Schwann cell differentiation and myelin synthesis in the adult. Better use of this time window may be a starting point for therapeutic strategies where remyelination fails.

METHODS

Methods and any associated references are available in the [online version of the paper](#).

Note: Supplementary information is available in the [online version of the paper](#).

ACKNOWLEDGMENTS

We thank C. Birchmeier (Max Delbrück Center, Berlin) for providing NRG1 'floxed' mice, L. Role (Stony Brook University) for providing NRG1 type III mutants, and A. Fahrenholz for help with immunohistochemistry. This work was supported by grants from Deutsche Forschungsgemeinschaft Research Center Molecular Physiology of the Brain, European Commission FP7-201535 (Ngidd) to K.-A.N. and by the Association Française contre Les Myopathies (15037 to M.W.S.). M.W.S. and R.F. were supported by the German Ministry of Education and Research (BMBF, FKZ: 01ES0812 to M.W.S.). M.W.S. is funded through a Deutsche Forschungsgemeinschaft Heisenberg professorship. K.-A.N. is funded through a European Research Council Advanced Investigator grant.

AUTHOR CONTRIBUTIONS

R.M.S. and R.F. performed experiments. V.V. performed immunohistochemistry analyses. B.G.B. and D.M. generated transgenic mice. R.M.S., M.W.S., M.H.S. and K.-A.N. supervised the work. R.M.S., M.W.S. and K.-A.N. wrote the manuscript.

COMPETING FINANCIAL INTERESTS

The authors declare no competing financial interests.

Published online at <http://www.nature.com/doi/10.1038/nn.3281>.

Reprints and permissions information is available online at <http://www.nature.com/reprints/index.html>.

- Jessen, K.R. & Mirsky, R. The origin and development of glial cells in peripheral nerves. *Nat. Rev. Neurosci.* **6**, 671–682 (2005).
- Nave, K.A. Myelination and support of axonal integrity by glia. *Nature* **468**, 244–252 (2010).
- Taveggia, C., Feltri, M.L. & Wrabetz, L. Signals to promote myelin formation and repair. *Nat. Rev. Neurol.* **6**, 276–287 (2010).
- Michailov, G.V. *et al.* Axonal neuregulin-1 regulates myelin sheath thickness. *Science* **304**, 700–703 (2004).
- Taveggia, C. *et al.* Neuregulin-1 type III determines the ensheathment fate of axons. *Neuron* **47**, 681–694 (2005).
- Nave, K.A. & Salzer, J.L. Axonal regulation of myelination by neuregulin 1. *Curr. Opin. Neurobiol.* **16**, 492–500 (2006).
- Birchmeier, C. & Nave, K.A. Neuregulin-1, a key axonal signal that drives Schwann cell growth and differentiation. *Glia* **56**, 1491–1497 (2008).
- Falls, D.L. Neuregulins and the neuromuscular system: 10 years of answers and questions. *J. Neurocytol.* **32**, 619–647 (2003).
- Bosse, F. Extrinsic cellular and molecular mediators of peripheral axonal regeneration. *Cell Tissue Res.* **349**, 5–14 (2012).
- Atanosoki, S. *et al.* ErbB2 signaling in Schwann cells is mostly dispensable for maintenance of myelinated peripheral nerves and proliferation of adult Schwann cells after injury. *J. Neurosci.* **26**, 2124–2131 (2006).
- Fricker, F.R. *et al.* Axonally derived neuregulin-1 is required for remyelination and regeneration after nerve injury in adulthood. *J. Neurosci.* **31**, 3225–3233 (2011).
- Fricker, F.R. & Bennett, D.L. The role of neuregulin-1 in the response to nerve injury. *Future Neurol.* **6**, 809–822 (2011).
- Sherman, D.L. & Brophy, P.J. Mechanisms of axon ensheathment and myelin growth. *Nat. Rev. Neurosci.* **6**, 683–690 (2005).
- Schröder, J.M. Altered ratio between axon diameter and myelin sheath thickness in regenerated nerve fibers. *Brain Res.* **45**, 49–65 (1972).
- Jaegle, M. *et al.* The POU proteins Brn-2 and Oct-6 share important functions in Schwann cell development. *Genes Dev.* **17**, 1380–1391 (2003).
- Li, L. *et al.* The breast proto-oncogene, HRGalpha regulates epithelial proliferation and lobuloalveolar development in the mouse mammary gland. *Oncogene* **21**, 4900–4907 (2002).
- Fawcett, J.W. & Keynes, R.J. Peripheral nerve regeneration. *Annu. Rev. Neurosci.* **13**, 43–60 (1990).
- Welcher, A.A., Suter, U., De Leon, M., Bitler, C.M. & Shooter, E.M. Molecular approaches to nerve regeneration. *Phil. Trans. R. Soc. Lond. B* **331**, 295–301 (1991).
- Bermingham-McDonogh, O., Xu, Y.T., Marchionni, M.A. & Scherer, S.S. Neuregulin expression in PNS neurons: isoforms and regulation by target interactions. *Mol. Cell. Neurosci.* **10**, 184–195 (1997).
- Carroll, S.L., Miller, M.L., Frohnert, P.W., Kim, S.S. & Corbett, J.A. Expression of neuregulins and their putative receptors, ErbB2 and ErbB3, is induced during Wallerian degeneration. *J. Neurosci.* **17**, 1642–1659 (1997).
- Wolpowitz, D. *et al.* Cysteine-rich domain isoforms of the neuregulin-1 gene are required for maintenance of peripheral synapses. *Neuron* **25**, 79–91 (2000).
- Myers, R.R. *et al.* Inhibition of p38 MAP kinase activity enhances axonal regeneration. *Exp. Neurol.* **184**, 606–614 (2003).
- Mirsky, R. *et al.* Novel signals controlling embryonic Schwann cell development, myelination and dedifferentiation. *J. Peripher. Nerv. Syst.* **13**, 122–135 (2008).
- Jessen, K.R. & Mirsky, R. Negative regulation of myelination: relevance for development, injury, and demyelinating disease. *Glia* **56**, 1552–1565 (2008).
- Höke, A. Mechanisms of disease: what factors limit the success of peripheral nerve regeneration in humans? *Nat. Clin. Pract. Neurol.* **2**, 448–454 (2006).
- Chen, Z.L., Yu, W.M. & Strickland, S. Peripheral regeneration. *Annu. Rev. Neurosci.* **30**, 209–233 (2007).
- Napoli, I. *et al.* A central role for the ERK-signaling pathway in controlling Schwann cell plasticity and peripheral nerve regeneration *in vivo*. *Neuron* **73**, 729–742 (2012).
- Loeb, J.A., Khurana, T.S., Robbins, J.T., Yee, A.G. & Fischbach, G.D. Expression patterns of transmembrane and released forms of neuregulin during spinal cord and neuromuscular synapse development. *Development* **126**, 781–791 (1999).
- Rosenbaum, C. *et al.* Schwann cells express NDF and SMDF/n-ARIA mRNAs, secrete neuregulin, and show constitutive activation of erbB3 receptors: evidence for a neuregulin autocrine loop. *Exp. Neurol.* **148**, 604–615 (1997).
- Stoneypher, M.S., Chaudhury, A.R., Byer, S.J. & Carroll, S.L. Neuregulin growth factors and their ErbB receptors form a potential signaling network for schwannoma tumorigenesis. *J. Neuropathol. Exp. Neurol.* **65**, 162–175 (2006).
- Pertusa, M., Morenilla-Palao, C., Carteron, C., Viana, F. & Cabedo, H. Transcriptional control of cholesterol biosynthesis in Schwann cells by axonal neuregulin 1. *J. Biol. Chem.* **282**, 28768–28778 (2007).
- Velanac, V. *et al.* Bace1 processing of NRG1 type III produces a myelin-inducing signal but is not essential for the stimulation of myelination. *Glia* **60**, 203–217 (2012).

ONLINE METHODS

Mutant and transgenic mice. The generation and genotyping of C57Bl6-Tg(*Thy1-Nrg1*III*)1*Kan*^{+/−}, C57Bl6-Tg(*Thy1-Nrg1*I*)1*Kan*^{+/−}, C57Bl6-(*Nrg1*^{tm2Cbm}) mice and C57Bl6-*Nrg1*^{tm1Lwr} mice has been described^{4,16,21}. The *Dhh-Cre* driver line (C57Bl6-Tg(*Dhh-cre*)1Mejr) was also genotyped as described¹⁵. For PCR, we isolated genomic DNA from tail biopsies, using Invisorb Spin tissue Mini Kit (Invitex), according to the manufacturer's directions. For routine genotyping, we used PCR primers in a coamplification reaction. Primer sequences are available upon request. All animal experiments were approved and carried out in compliance with the guidelines of the Max Planck Institute of Experimental Medicine.

Nerve crush experiments. Adult mice at the age of 3 months were anesthetized with ketaminhydrochloride and xylazinhydrochloride (100 mg/kg body weight and 8 mg/kg body weight) and the sciatic nerve was exposed. The nerve was crushed at the mid-femoral level by a standardized compression with artery forceps for 40 s. The crush site was marked with an endoneurial suture. The mice were killed 0.5 d, 1 d, 4 d, 7 d, 14 d or 28 d after surgery, and their sciatic nerves and spinal cords were isolated and processed for histology, mRNA expression and protein expression analyses. For histology, the sciatic nerve was analyzed 4 mm distal to the crush injury site. The spinal cord was dissected from the first to the second lumbar segment (L1–L2), and mRNA expression analysis was performed with the ipsilateral and contralateral ventral quadrant, whereas cross-sections where used for immunohistochemistry. Pharmacological experiments were performed by intraneural injection of 5 μ l carrier solution into the distal part of injured sciatic nerves using a glass capillary and hand-held Hamilton syringe (Hamilton-Bonaduz).

Electron microscopy and morphometry. Mice were perfused with 4% paraformaldehyde and 2.5% glutaraldehyde in 0.1 M PBS. Sciatic nerves were removed, contrasted with osmium tetroxide and Epon-embedded. Semithin cross-sections (0.5 μ m) were cut using a microtome (Leica, RM 2155) with a diamond knife (Histo HI 4317, Diatome). Sections were stained with azur II-methylenblue for 1 min at 60 °C. Light microscopy observations were carried out with a \times 100 lens (Leica DMRXA), and images were digitalized and analyzed with Openlab 3.1.1 and Scion Image software. Axonal counts and counting of Schwann cell numbers were performed on total sciatic nerve cross section. For electron microscopy analysis of sciatic nerves, ultrathin (50–70 nm) cross-sections were stained with 1% uranyl acetate solution and 2.66% lead nitrate and analyzed using a Zeiss EM10 or EM109 Leo. The *g* ratio was determined by dividing the circumference of an axon (without myelin) by the circumference of the same axon including myelin sheath. At least 100 fibers per mouse were analyzed. Axon and Schwann cell counts were performed on ten randomized electron microscopy pictures with a total area of 8,247 μ m².

Immunohistochemistry. For standard immunohistochemical analysis, mice were perfused with 4% PFA in 0.1 M phosphate buffer. Dissected sciatic nerve and spinal cord tissue was imbedded in paraffin. Teased fibers were prepared and immunostained as described in ref. 33. Sections or samples were incubated overnight with primary antibodies to NRG1 (pRb; 1:250, Santa Cruz SC-348), EGR2 (pRb; 1:400 (ref. 34)), KI-67 (mRb; 1:100, Dako), POU3f1 (pRb; 1:500 (ref. 34)) MBP (mM; 1:200, Covance), Na_v1.6 (pRb; 1:250, Alomone), S100 (mM; 1:250, Millipore) and MPZ (mM; 1:1,000; gift from J. Archelos). Samples were then incubated with secondary cyanine dyes (1:1,000, Jackson ImmunoResearch) for 1 h at room temperature. For 3,3'-diaminobenzidine (DAB)-based immunostaining (KI-67), the Dako-LSAB₂ kit was used according to the manufacturer's instructions. Complete cross-sections of the sciatic nerve were analyzed. Digital images of stained sections and teased fiber preparations were obtained by light microscopy (Zeiss Axiophot or using a confocal laser scanning microscope, Leica DM RXA) and Openlab 3.1.1 software (Improvision). Images were processed by using US National Institutes of Health ImageJ, Photoshop CS (Adobe) and Illustrator 10 (Adobe).

RNA analysis. Total RNA was extracted using Qiazol Reagent according to the manufacturer's instructions (Qiagen). The integrity of purified RNA was confirmed using the Agilent 2100 Bioanalyser (Agilent Technologies). For reverse-transcriptase (RT)-PCR analysis, cDNA was synthesized from total RNA using

random nonamer primers and Superscript III RNase H reverse transcriptase (Invitrogen). Quantitative real-time PCR was carried out using the Roche LC480 Detection System and SYBR Green Master Mix according to the manufacturer (Applied Biosystems). Reactions were carried out at least in triplicate. The relative quantity of RNA was calculated using 7500 Fast System SDS software version 1.3 (Applied Biosystems). Results were depicted as histograms (generated using Microsoft Excel 2003) of normalized relative quantity values, with mean relative quantity value in the given control group normalized to 100%. As internal standards, actin beta (*Actb*), peptidylprolyl isomerase A (*Ppia*) and ribosomal protein, large, P0 (*Rplp0*) were used. PCR primer sequences are available upon request.

Protein analysis. Cultured cells were collected in lysis buffer (1% SDS in 0.1 M PBS with protease inhibitors (Complete; Roche)), whereas sciatic nerve samples were lysed in sucrose buffer (320 mM sucrose, 10 mM Tris, 1 mM NaHCO₃ and 1 mM MgCl₂) containing protease inhibitors (Complete Roche) and phosphatase inhibitors (PhosSTOP Roche). Detection of immunolabeled protein was performed using chemiluminescence (NEN Life Science Products). Representative results from at least three independent experiments are shown. Western blots were incubated overnight with primary antibodies to NRG1 (pRb; 1:500, Santa Cruz SC-348), ERBB2 (pRb; 1:500, Santa Cruz SC-284), p-ERBB2 (pRb; 1:500, Santa Cruz SC-293110), ERK1/2 (pRb; 1:2,000, Cell Signaling #4695), p-ERK1/2 (pRb; 1:2,000, Cell Signaling #4370), GAPDH (mM; 1:5,000, Stressgen) and alpha tubulin (mM; 1:5000, SIGMA).

Primary cell culture. Rat Schwann cells were prepared from sciatic nerves of newborn rats (1–2 d old) as described previously³⁵. For mimicking a denervated Schwann cell phenotype, cells were kept in minimal medium (DMEM (Gibco) with 5% FCS) and analyzed within 5 d after preparation. Cell media were then supplied with 20 ng per ml medium recombinant human Neuregulin-1 beta EGF like domain (EGF-1d, Reprokin). Blocking experiments were performed using the specific ERBB2 inhibitor II (Santa Cruz), MAP kinase inhibitor U0126 (Cell Signaling), PI3 kinase inhibitor LY294002 (Cell Signaling) and the calcineurin signaling inhibitor cyclosporin A (Ascent Scientific), which were added to the medium 2 h before Neuregulin-1 beta treatment. For analysis of primary rat Schwann cells with axonal contact, cells were added to the neuron-free compartments of Campenot chambers into which the axons of primary DRG neurons had grown³⁶. Primary DRG neuron cultures were obtained from mouse embryos at embryonic day 13 as described in ref. 37.

Electrophysiology. Electrophysiology was performed on control mice (intact nerve) and after nerve crush injury (remyelinated nerve). Mice were anesthetized with ketaminhydrochloride and xylazinhydrochloride (100 mg/kg body weight and 8 mg/kg body weight). A pair of steel needle electrodes (Schuler Medizintechnik) was placed subcutaneously along the nerve at sciatic notch (proximal stimulation). A second pair of electrodes was placed along the tibial nerve above the ankle (distal stimulation). Supramaximal square wave pulses lasting 100 ms were delivered using a Toennies Neuroscreen (Jaeger). Compound muscle action potential (CMAP) was recorded from the intrinsic foot muscles using steel electrodes. Both amplitudes and latencies of CMAP were determined. The distance between the two sites of stimulation was measured alongside the skin surface with fully extended legs, and nerve conduction velocities (NCVs) were calculated automatically from sciatic nerve latency measurements.

Walking track analysis: sciatic functional index (SFI). The hind paws of each mouse were moistened with water-soluble, nontoxic ink and the mice were allowed to walk unassisted along a corridor lined with white paper. Five prints of each foot were selected for measurements at a point when the mouse was walking at a moderate pace. The parameters toe spread and paw print length from the intact and injured side were assessed to calculate the SFI as described³⁸.

Statistical analysis. Data are expressed in mean \pm s.e.m. unless indicated otherwise. Statistical differences over all groups were determined using either the nonparametric Mann-Whitney *U* test or the Student's *t*-test. Statistical differences were considered to be significant for *P* < 0.05 (**P* < 0.05, ***P* < 0.01, ****P* < 0.001). All statistical analysis was performed using the software Statistica 10.0 (StatSoft).

33. Spiegel, I. *et al.* A central role for Necl4 (SynCAM4) in Schwann cell-axon interaction and myelination. *Nat. Neurosci.* **10**, 861–869 (2007).
34. Ghazvini, M. *et al.* A cell type-specific allele of the POU gene Oct-6 reveals Schwann cell autonomous function in nerve development and regeneration. *EMBO J.* **21**, 4612–4620 (2002).
35. Brockes, J.P., Fields, K.L. & Raff, M.C. Studies on cultured rat Schwann cells. I. Establishment of purified populations from cultures of peripheral nerve. *Brain Res.* **165**, 105–118 (1979).
36. Campenot, R.B. Development of sympathetic neurons in compartmentalized cultures. II Local control of neurite growth by nerve growth factor. *Dev. Biol.* **93**, 1–12 (1982).
37. Kleitman, N., Wood, P.M. & Bunge, R.P. Tissue culture methods for the study of myelination. in *Culturing Nerve Cells* 2nd edn. (eds., Banker G.A. & Goslin, K.) 545–594 (MIT, 1998).
38. Inserra, M.M., Bloch, D.A. & Terris, D.J. Functional indices for sciatic, peroneal, and posterior tibial nerve lesions in the mouse. *Microsurgery* **18**, 119–124 (1998).